

FLEXURAL BEHAVIOUR IN PRESTRESSED RUBBER CONCRETE SLEEPERS WITH RECYCLED AGGREGATE

Setkit, M.^{*,**}; Imjai, T.^{*,**}; Rahim, N. L.^{***} & Leelatanon, S.^{*,**,#}

^{*} School of Engineering and Technology, Walailak University, Thasala, Nakhon Si Thammarat 80160, Thailand

^{**} Centre of Excellence in Sustainable Disaster Management, Walailak University, Thasala, Nakhon Si Thammarat 80160, Thailand

^{***} Faculty of Civil Engineering and Technology, Universiti Malaysia Perlis, 02600, Arau, Perlis, Malaysia

E-Mail: lsatjapa@wu.ac.th (# Corresponding author)

Abstract

This paper investigates the structural performance and mix optimisation of prestressed concrete sleepers incorporating recycled concrete aggregate (RCA) and crumb rubber (CR). Nine mix proportions of full-scale sleepers were tested in four-point bending under three regimes including centre positive, rail-seat positive, and rail-seat negative. Load-deflection responses were processed to obtain ultimate load, initial stiffness, energy absorbed to peak, and deflection at peak. Quadratic response-surface models were fitted to RCA and CR contents and combined with a multi-response desirability approach to identify compromise-optimal mixtures balancing capacity, stiffness, toughness, and sustainability. Results show that increasing RCA causes modest, smooth reductions in strength and stiffness, with no abrupt thresholds up to 50 % replacement, while peak deflection remains largely unchanged and absorbed energy follows the strength trend. CR introduces a controlled strength-ductility trade-off, enhancing toughness and peak deflection at moderate penalties to capacity and stiffness. Optimisation highlights a practical corridor centred on 25 % RCA with 4 % CR across all regimes.

(Received in October 2025, accepted in January 2026. This paper was with the authors 3 weeks for 1 revision.)

Key Words: Recycled Aggregate, Crumb Rubber, Prestressed Concrete Sleeper, Response Surface Methodology

1. INTRODUCTION

The escalating environmental burden posed by conventional construction practices necessitates a global paradigm shift toward sustainable engineering solutions. The construction sector remains the largest consumer of natural resources, utilizing approximately 12.6 billion tonnes of raw materials annually, while simultaneously generating vast amounts of construction and demolition waste [1]. Addressing this duality, the incorporation of waste materials, specifically recycled concrete aggregate (RCA) and crumb rubber (CR), into concrete production has become a critical research priority [2, 3].

RCA derived from construction and demolition waste serves to conserve finite natural resources [4]. However, the presence of residual adhered mortar in RCA typically results in increased porosity leading to a general reduction in the mechanical strength and durability of recycled aggregate concrete (RAC) [2, 5]. To better understand these complexities, novel theoretical frameworks such as fractal-based approaches have recently been introduced to characterize the mechanical properties of recycled aggregate concrete [6]. Simultaneously, crumb rubber (CR) from shredding waste vehicle tyres offers a viable solution to the accumulation of non-biodegradable rubber waste, nearly 1 billion of which are generated annually [7, 8].

The substitution of natural aggregates (NA) with CR, typically replacing fine aggregates, introduces a complex trade-off in concrete performance. While studies consistently show that increasing CR content generally leads to a reduction in mechanical properties such as

compressive, tensile, and flexural strengths, with strength reductions potentially exceeding 50 % in certain mixes, CR imparts critical advantages [9]. Conversely, CR significantly enhances dynamic properties, including ductility, toughness, impact resistance, and damping capacity, making it highly suitable for applications subjected to repetitive dynamic loads. Research has progressed to developing hybrid recycled aggregate-rubberized concrete that simultaneously incorporates both RCA and CR [10, 11].

This material combination is highly pertinent for critical infrastructure components such as prestressed concrete railway sleepers which must exhibit exceptional resilience and durability [12]. Previous investigations have established the feasibility of utilizing RCA in high-performance prestressed concrete sleepers [13, 14]. Furthermore, the desirable vibration absorption characteristics provided by CR position rubberized RAC as a promising material for robust railway systems [15, 16]. Concurrently, recent advancements have also demonstrated the efficacy of concrete canvas in enhancing the performance of railway substructures under static and dynamic loading conditions [17]. Similarly, studies on hybrid materials, such as steel-fibre-reinforced recycled aggregate concrete containing crumb rubber, highlight their suitability for flexural elements [18-20].

To effectively navigate the variable performance characteristics resulting from using hybrid waste aggregates (RCA and CR), advanced data-driven modelling techniques are required. Response surface methodology (RSM) is a statistical tool successfully employed in concrete research to model and optimise processes where complex interaction effects between multiple input factors influence the outcome [21, 22]. RSM has been effectively utilised for optimising hybrid concrete blends, including those containing crumb rubber and metakaolin, aiding in the prediction of material characteristics [9].

Despite these advancements, a critical research gap remains: the comprehensive data-driven simulation of the structural flexural behaviour of prestressed concrete sleepers explicitly engineered with the hybrid RCA-CR aggregate blend. Advanced computational strategies, including neural network identification, have been successfully applied to determine structural parameters in complex infrastructure like concrete bridges [23]. However, current research often focuses on material-level mechanical property prediction or generalised structural analyses, lacking a dedicated framework to accurately simulate the complex structural flexural response. Such a framework is needed to synthesize RCA variability and the strength-ductility balance of CR within a prestressed system [11, 24].

Therefore, the motivation of this study is to establish a reliable simulation tool capable of predicting the performance of sustainable railway components. The primary objective is to utilise a data-driven framework, informed by experimental optimisation principles, to develop and validate a simulation model that precisely predicts the load-deflection behaviour and ultimate flexural capacity of prestressed concrete railway sleepers incorporating varying volumetric substitution ratios of RCA and CR. The novelty of this work lies in delivering a data-driven simulation approach specifically tailored for predicting the complex structural flexural performance of prestressed concrete railway sleepers containing this unique hybrid waste material blend, thereby facilitating optimal and sustainable infrastructure design.

2. MATERIALS AND METHODS

2.1 Prestressed concrete sleepers

The concrete mixture consisted of 550 kg/m³ of Portland cement, 1,050 kg/m³ of coarse aggregate, and 850 kg/m³ of fine aggregate. The water-to-cement (w/c) ratio was maintained at 0.30 (167 kg/m³ of water), and a superplasticiser was added at a dosage of 8.25 kg/m³ (1.5 % by weight of cement). A portion of the fine aggregate was substituted by crumb rubber obtained from end-of-life tyres which have particle size of 0.15–4.75 mm and specific gravity of 0.95 as

shown in Fig. 1 a. Concurrently, recycled concrete aggregate characterized by an average size of 12.7 mm and a specific gravity of 2.45 was utilised to replace part of the coarse aggregate as presented in Fig. 1 b. The variables consisted of three replacement levels of RCA for coarse aggregate (0 %, 25 %, and 50 %) and three replacement levels of CR for fine aggregate (0 %, 4 %, and 8 %). This design matrix includes nine distinct mix proportions, as shown in Table I.



Figure 1: a) crumb rubber, b) recycled concrete aggregate.

Table I: Concrete mixture proportions (kg/m^3).

Mixture	Cement	Natural coarse aggregate	Recycled coarse aggregate	Fine aggregate	Crumb rubber	Water
N-C0	550	1050	0	850	0	167
N-C4	550	1050	0	837.25	12.75	167
N-C8	550	1050	0	824.5	25.5	167
R25-C0	550	787.5	262.5	850	0	167
R25-C4	550	787.5	262.5	837.25	12.75	167
R25-C8	550	787.5	262.5	824.5	25.5	167
R50-C0	550	525	525	850	0	167
R50-C4	550	525	525	837.25	12.75	167
R50-C8	550	525	525	824.5	25.5	167

Full-scale prestressed concrete sleeper specimens were fabricated with geometry adhering to the design standards of the State Railway of Thailand, as shown in Fig. 2. Each sleeper was prestressed using 20 high-tensile steel strands (4 mm in diameter) conforming to ASTM A416 Grade 270. These strands were tensioned to approximately 1,200 MPa prior to casting, achieving an effective force of about 75 % of the strand ultimate tensile strength.

2.2 Test setup

The structural performance of each concrete mixture was evaluated using three distinct bending test configurations designed to simulate critical in-service loading conditions, including centre positive, rail-seat positive, and rail-seat negative moments. All tests maintained statically determinate conditions via pinned-roller supports. As shown in Fig. 3, the centre positive moment test involved supporting the specimen at the rail-seats (1,070 mm span) under a mid-span load. For the rail-seat positive moment, the load was applied 330 mm from the support. Conversely, for the rail-seat negative moment, the specimen was inverted, with the load similarly applied 330 mm from the support to induce maximum negative moment.

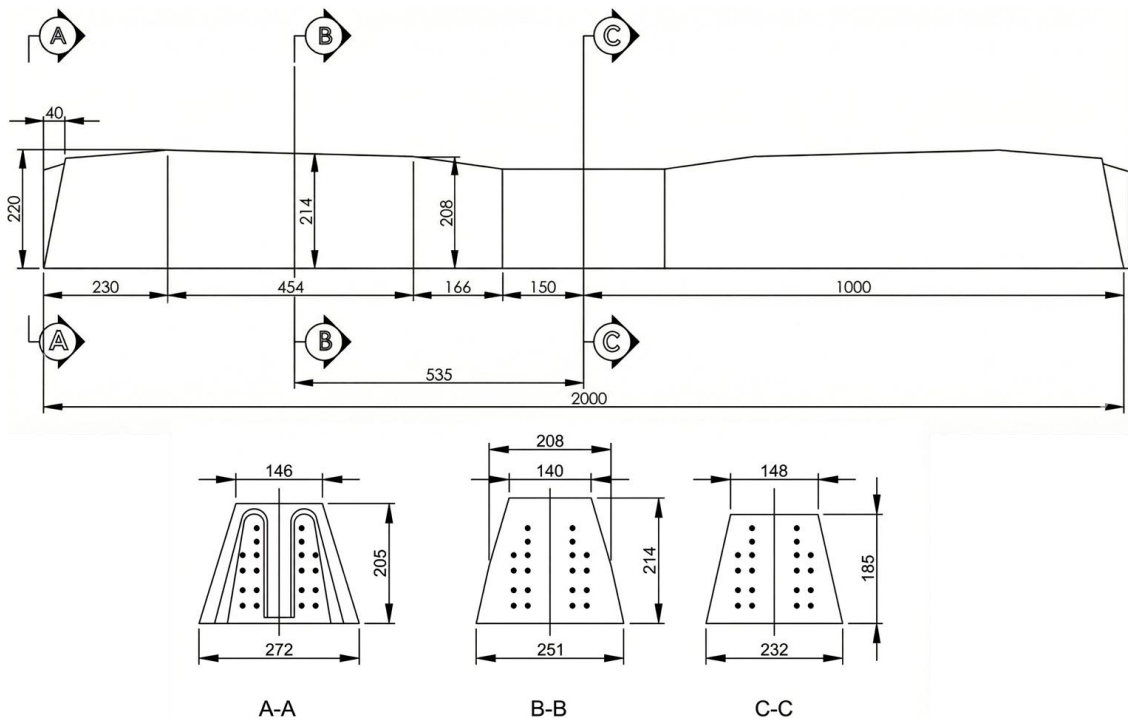


Figure 2: Dimensions of prestressed concrete sleeper specimens.

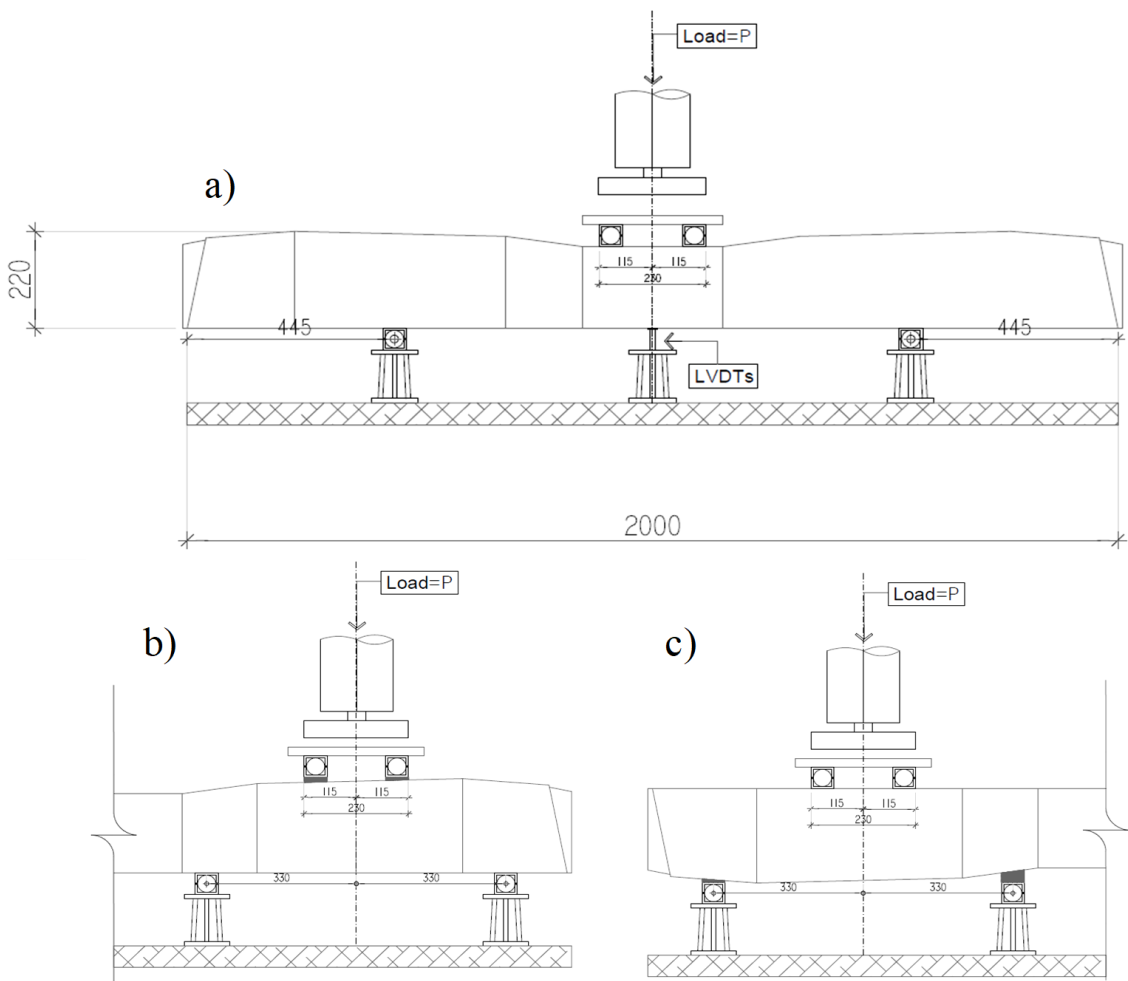


Figure 3: Three loading configurations; a) centre positive moment, b) seat positive moment, c) seat negative moment.

For all test configurations, load was applied by a servo-hydraulic testing machine through a 1,000 kN load cell. The practical loading increment was 2 kN/min. Linear variable differential transformers (LVDTs) were positioned at mid-span for the centre positive tests, and at each rail seat for the rail-seat tests. All data from load cell and LVDTs were synchronised and acquired through a computerised system at 2 Hz.

3. RESULT ANALYSIS AND DISCUSSION

3.1 Load-deflection curves of sleepers by static load tests

All analyses are conducted on the measured load-deflection curves from three bending tests including centre positive, rail-seat positive, and rail-seat negative. Each test was obtained on full-scale prestressed sleepers of 2,000 mm span with pinned-roller boundary conditions. All load-deflection of three bending tests are shown in Fig. 4. Four physically interpretable response variables are extracted from every curve and used consistently throughout:

- **Ultimate load** (P_u): the maximum recorded load prior to unloading or abrupt post-peak loss.
- **Initial stiffness** (k_0): the tangent stiffness identified by a linear least-squares fit to the initial elastic segment and bounded at 10–15 % of P_u to avoid micro-cracking non-linearity.
- **Energy to peak** (E_u): the mechanical work up to ultimate load estimated by trapezoidal integration under the load-deflection curve.
- **Deflection at peak** (Δ_u): the corresponding deflection at ultimate load.

Concrete sustainability variables are defined as continuous factors: recycled concrete aggregate replacement, r ($0\% \leq r \leq 50\%$) and crumb rubber content, c ($0\% \leq c \leq 8\%$).

3.2 Response-surface modelling (RSM)

To interpolate the discrete factorial design (N, R25, R50 \times C0, C4, C8) and to enable optimisation, a second-order response surface is adopted for each response $y \in \{P_u, k_0, E_u, \Delta_u\}$ and each test regime, written in the factors r and c .

$$y(r, c) = \beta_0 + \beta_1 r + \beta_2 c + \beta_{11} r^2 + \beta_{22} c^2 + \beta_{12} rc + \varepsilon \quad (1)$$

with ordinary least-squares estimation,

$$\hat{\beta} = (X^T X)^{-1} X^T y, \quad \hat{y} = X \hat{\beta} \quad (2)$$

where $X = [1, r, c, r^2, c^2, rc]$. The second-order form is the classical local surrogate recommended for experimental optimisation and factor interaction screening in engineering systems with limited but systematically acquired data. The linear terms β_1 and β_2 indicate marginal trends of RCA and CR. The quadratic terms β_{11} and β_{22} capture curvature (e.g., diminishing returns or softening at higher percentages) and β_{12} quantifies the interaction between RCA and CR.

3.3 Validation protocol and error metrics

Model adequacy is reported in-sample and by k -fold cross-validation (with k adapted to the number of aggregated mixes within each regime). For observed-predicted pairs $\{(y_i, \hat{y}_i)\}_{i=1}^n$:

$$RMSE = \sqrt{\frac{1}{n} \sum_{i=1}^n (y_i - \hat{y}_i)^2}, \quad MAE = \frac{1}{n} \sum_{i=1}^n |y_i - \hat{y}_i| \quad (3)$$

$$R^2 = 1 - \frac{\sum_{i=1}^n (y_i - \hat{y}_i)^2}{\sum_{i=1}^n (y_i - \bar{y})^2} \quad (4)$$

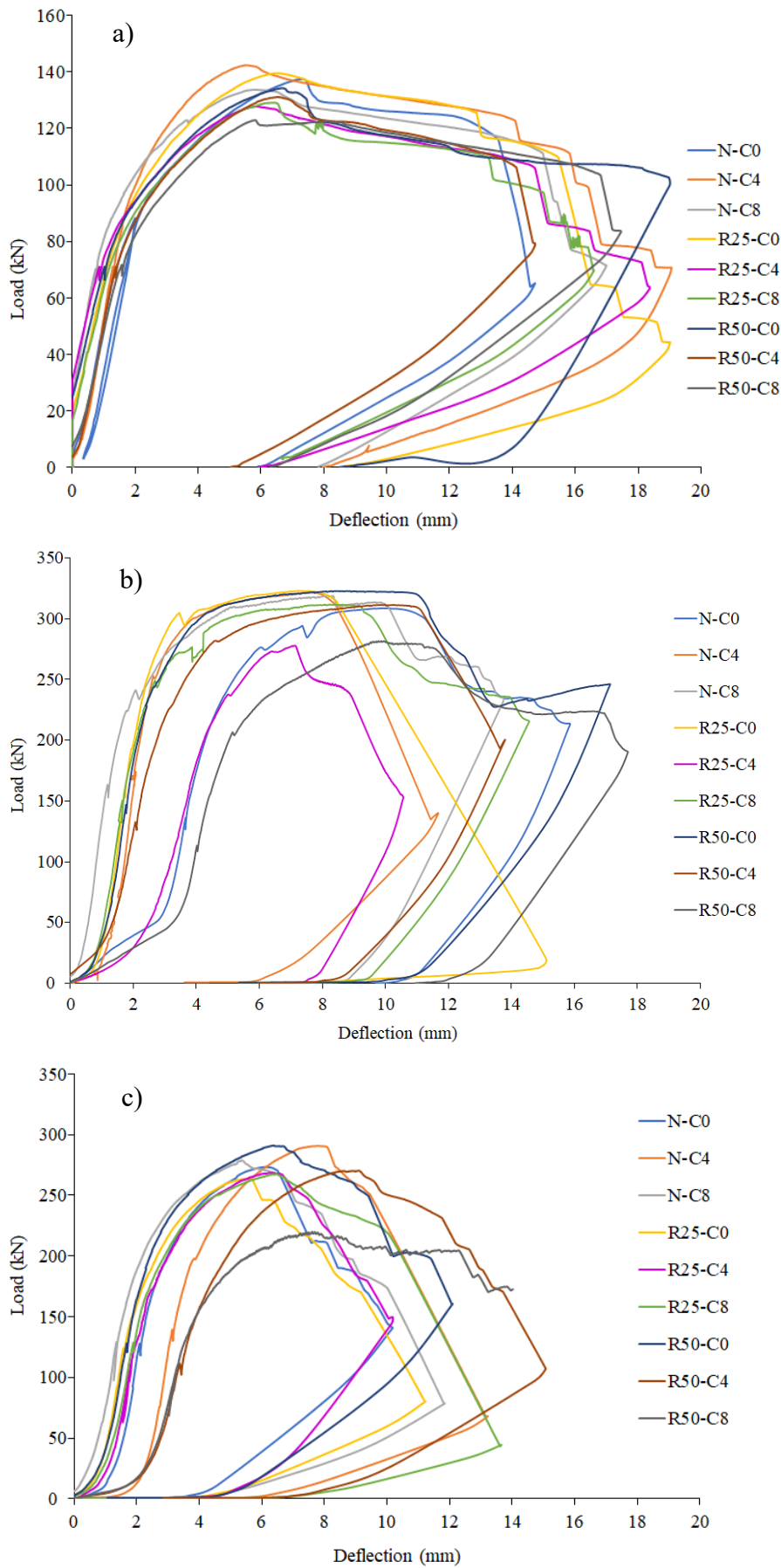


Figure 4: The relation of load-deflection of a) centre positive, b) rail-seat positive, c) rail-seat negative.

In cross-validation, the data set is partitioned into folds $\{\mathcal{F}_j\}_{j=1}^k$; refitting Eq. (1) on the complement and predicting on \mathcal{F}_j produces fold-wise scores that are averaged to obtain \overline{RMSE}_{cv} , \overline{MAE}_{cv} and $\overline{R^2}_{cv}$. Residual plots and influence diagnostics (Cook's distance) are screened to ensure no undue leverage by any single mix.

3.4 Multi-response desirability and compromise optimisation

Sleeper design requires balancing strength and stiffness against deformability, toughness and sustainability. Each response is mapped to an individual desirability $d \in [0, 1]$ following the Derringer–Suich convention with lower and upper acceptance bounds, L and U :

$$d(y) = \begin{cases} 0 & , y \leq L \\ \left(\frac{y-L}{U-L}\right)^s & , L < y < U \\ 1 & , y \geq U \end{cases} \quad (5)$$

with larger-is-better mapping for P_u , k_0 and E_u . A simple sustainability factor $d_{sust}(r, c) \in [0, 1]$ rewards higher RCA while discouraging excessive CR, e.g.

$$d_{sust}(r, c) = \left(\frac{r}{50}\right)^{s_r} \left(1 - \frac{c}{c_{max}}\right)^{s_c} \quad (6)$$

clamped to $[0, 1]$. The overall desirability aggregates the components by a weighted geometric mean:

$$D = (d_{P_u}^{w_1} d_{k_0}^{w_2} d_{E_u}^{w_3} d_{sust}^{w_4})^{\frac{1}{w_1+w_2+w_3+w_4}} \quad (7)$$

and is maximised over a grid $(r, c) \in [0, 50] \times [0, 8]$ to shortlist compromise-optimal mixes per regime. Default weights are $w_1 = 0.4$, $w_2 = 0.2$, $w_3 = 0.3$ and $w_4 = 0.1$. Sensitivity to weights is reported qualitatively below. The three desirability surfaces $D(r, c)$ obtained from the fitted RSMs including centre positive, rail-seat positive and rail-seat negative are shown in Fig. 5.

3.5 Effect of recycled concrete aggregate and crumb rubber

Across all regimes, the linear RCA coefficient β_1 in Eq. (1) is mildly negative for P_u and k_0 , while the curvature β_{11} is small, as shown in Table II, indicating a gradual rather than threshold-type decline as r increases to 50%. The predicted reductions from R25 to R50 are modest and remain within the dispersion of the experimental replicates; importantly, Δ_u shows little systematic dependence on r alone, and E_u follows the trend of P_u . Mechanistically, this is consistent with the lowered aggregate modulus and weaker interfacial transition zone (ITZ) typically associated with RCA, whose influence at the member scale is partially offset by prestressing and reinforcement continuity.

The CR coefficient β_2 is negative for P_u and k_0 and positive for E_u and Δ_u with a non-linear response captured by $\beta_{22} > 0$. Physically, rubber particles are compliant inclusions that reduce the composite modulus and promote crack deflection and branching, thereby sacrificing peak stiffness and strength while raising energy absorption. This strength-ductility trade-off is most evident in the rail-seat regimes, where curvature and localised stresses reward deformability. The predicted E_u gains at C4 are substantial with tolerable penalties in P_u and k_0 ; however, by C8, while the toughness increases further, the stiffness penalty becomes operationally significant. The desirability surfaces in Fig. 5 reflect that contours of high D align with low CR

corridors where d_{E_u} is already elevated but d_{k_0} and d_{P_u} have not yet eroded below the acceptance bounds (L) in Eq. (5).

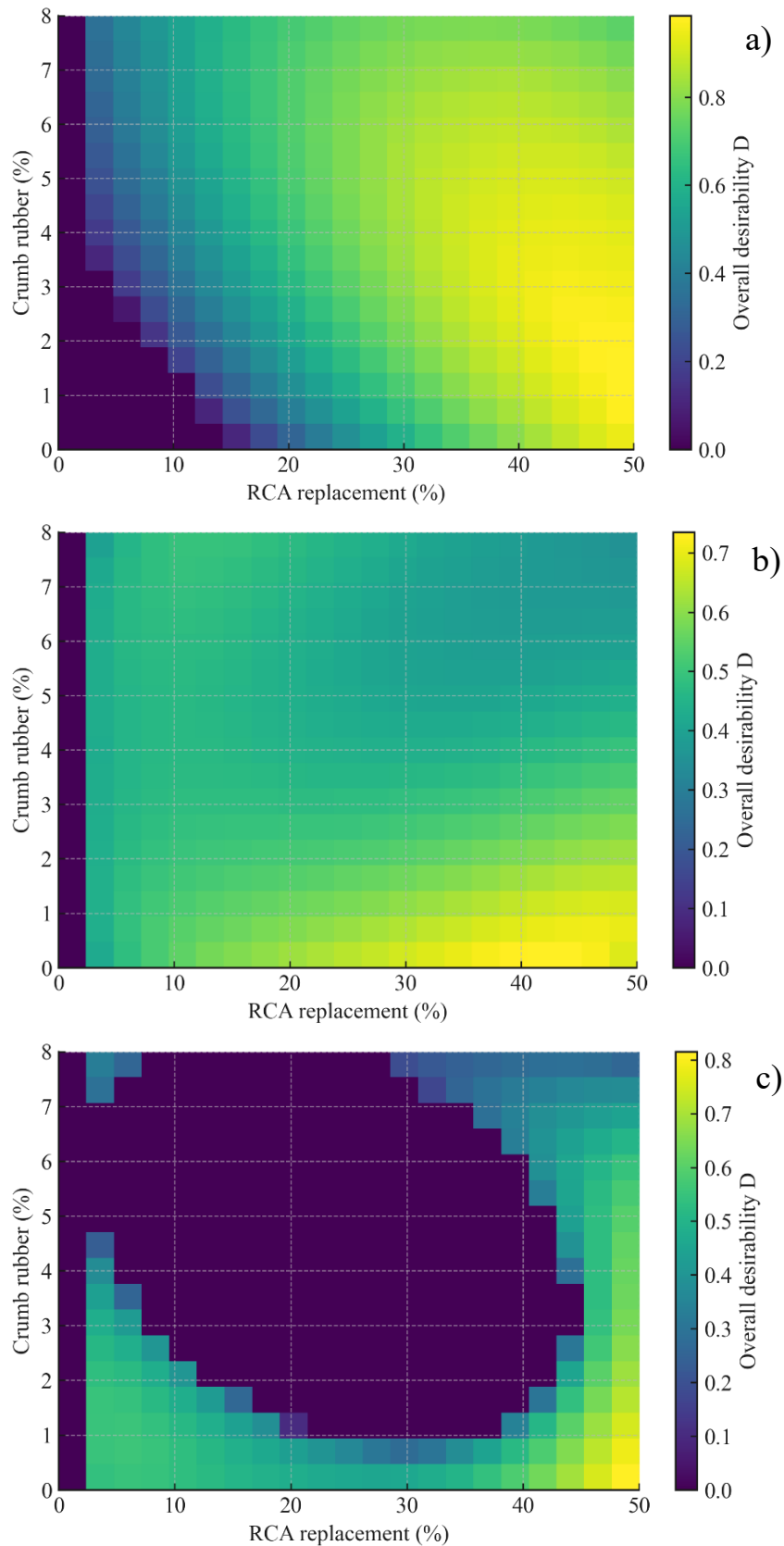


Figure 5: Three desirability surfaces (D) obtained from a) centre positive, b) rail-seat positive, c) rail-seat negative.

Table II: Quadratic RSM coefficients (β) by regime and response.

Regime	Response	β_0	β_1 (RCA)	β_2 (CR)	β_{11} (RCA ²)	β_{22} (CR ²)	β_{12} (RCA×CR)	RMSE	R ²
Centre Positive	P_u	55.6	3.5	4.29	-0.0385	0.0195	-0.125	2.66	0.982
	k_0	-3180	21.0	944.0	0.641	-61.6	-8.05	426.0	0.786
	E_u	-204	26.1	104.0	-0.199	-5.55	-1.51	19.0	0.987
	Δ_u	3.79	0.0888	0.569	-0.00043	-0.024	-0.00898	0.143	0.937
Rail Seat Positive	P_u	325.0	-0.914	-6.42	0.0165	0.689	-0.0698	10.6	0.608
	k_0	-1.49	0.124	0.307	-0.00235	-0.043	0.00125	1.03	0.374
	E_u	1480	-11.1	-39.2	0.45	15.2	-2.65	311.0	0.414
	Δ_u	6.84	-0.057	-0.016	0.00201	0.0406	-0.0034	0.802	0.672
Rail Seat Negative	P_u	262.0	0.357	9.37	-0.00015	-0.902	-0.188	7.24	0.875
	k_0	11.4	-0.596	-3.37	0.00946	0.283	0.0341	1.19	0.906
	E_u	948	-19.3	107.0	0.479	-14.0	-0.892	74.5	0.897
	Δ_u	6.59	-0.116	0.938	0.00263	-0.119	-0.00163	0.849	0.697

Note: P_u in kN, k_0 in kN/mm, E_u in kN·mm and Δ_u in mm respectively.

The interaction term β_{12} in Eq. (1) is mild but consistent across regimes. At higher CR, the incremental penalty of RCA on P_u and k_0 is slightly amplified, whereas at low CR the marginal effect of RCA is comparatively small. Consequently, the combined RSM in Eq. (1) and desirability rule in Eq. (7) produce ridge-like optima in the (r , c) plane. For all three regimes, the maxima of D fall in the vicinity of R25-C4, with R50-C4 emerging as an acceptable variant when sustainability weighting w_4 is emphasised. This behaviour is clearly visible in Fig. 5, where the warm-coloured plateaus align near $c = 4\%$ and r in the range of 25–50%.

4. CONCLUSION

This study combined full-scale four-point bending tests on prestressed concrete sleepers with response-surface modelling and multi-response desirability to quantify and balance the roles of recycled concrete aggregate and crumb rubber. From each load-deflection record, four design-relevant indices were extracted: ultimate load, initial stiffness, energy absorbed up to peak, and deflection at peak.

Recycled aggregate produced modest, smooth reductions in ultimate load and initial stiffness as the replacement level increased, with no abrupt thresholds within the tested window up to one-half replacement by weight. Deflection at peak was largely insensitive, and absorbed energy followed the overall strength trend. These observations indicate that recycled aggregate can serve as a primary sustainability lever in prestressed sleepers, where prestressing and reinforcement continuity help maintain global performance.

Crumb rubber introduced a clear strength-ductility trade-off. Small additions increased toughness and peak deflection while imposing only moderate penalties on capacity and stiffness. Approximately 4% replacement of natural sand with crumb rubber yielded the most attractive balance across regimes; at 8%, while the toughness benefit remained, the stiffness penalty became operationally significant for serviceability, especially at the rail seat where curvature demands are higher.

When recycled aggregate and crumb rubber were used together, the interaction was present but not dominant. At higher crumb levels, the incremental penalty of recycled aggregate on capacity and stiffness was slightly amplified. Desirability maps that emphasised capacity and

toughness, while incorporating a sustainability bonus, consistently highlighted a practical corridor centred on 25 % recycled aggregate with 4 % crumb rubber; extending recycled aggregate to 50 % remained feasible when sustainability weighting was prioritised.

For implementation, factory trials are recommended using the 25 % recycled aggregate and 4 % crumb rubber blend, with targeted verification at centre and rail-seat locations. Generalisation beyond the tested ranges and long-term effects such as fatigue, creep and shrinkage warrant future programmes, but the present evidence shows that sustainable constituents can be deployed in prestressed sleepers without compromising structural adequacy when crumb rubber is moderated and recycled aggregate is the principal replacement lever.

Future investigations should focus on optimising the synergy of recycled concrete aggregates, crumb rubber, and supplementary fibre reinforcement in sleepers to offset strength and stiffness losses while substantially improving toughness and energy absorption. Key directions include exploring hybrid fibre reinforcement and surface treatments of recycled aggregates to enhance bonding and mechanical properties. Additionally, long-term fatigue performance studies and full-scale manufacturing trials are needed to validate durability and serviceability.

ACKNOWLEDGEMENT

The authors wish to thank the Thailand Science Research and Innovation for supporting research fund (Contract No. FF-WU67-01). Additionally, the authors would like to thank the undergraduate students in Civil Engineering at Walailak University for their assistance with the experimental work of this research.

REFERENCES

- [1] Hossain, F. M. Z.; Shahjalal, M.; Islam, K.; Tiznobaik, M.; Alam, M. S. (2019). Mechanical properties of recycled aggregate concrete containing crumb rubber and polypropylene fiber, *Construction and Building Materials*, Vol. 225, 983-996, doi:[10.1016/j.conbuildmat.2019.07.245](https://doi.org/10.1016/j.conbuildmat.2019.07.245)
- [2] Prasittisopin, L.; Tuvayanond, W.; Kang, T. H.-K.; Kaewunruen, S. (2025). Concrete mix design of recycled concrete aggregate (RCA): analysis of review papers, characteristics, research trends, and underexplored topics, *Resources*, Vol. 14, No. 2, Paper 21, 43 pages, doi:[10.3390/resources14020021](https://doi.org/10.3390/resources14020021)
- [3] Kazmi, S. M. S.; Munir, M. J.; Wu, Y.-F. (2021). Application of waste tire rubber and recycled aggregates in concrete products: a new compression casting approach, *Resources, Conservation and Recycling*, Vol. 167, Paper 105353, 14 pages, doi:[10.1016/j.resconrec.2020.105353](https://doi.org/10.1016/j.resconrec.2020.105353)
- [4] Alibeigibeni, A.; Stochino, F.; Zucca, M.; Gayarre, F. L. (2025). Enhancing concrete sustainability: a critical review of the performance of recycled concrete aggregates (RCAs) in structural concrete, *Buildings*, Vol. 15, No. 8, Paper 1361, 25 pages, doi:[10.3390/buildings15081361](https://doi.org/10.3390/buildings15081361)
- [5] Pedro, D.; de Brito, J.; Evangelista, L. (2017). Structural concrete with simultaneous incorporation of fine and coarse recycled concrete aggregates: mechanical, durability and long-term properties, *Construction and Building Materials*, Vol. 154, 294-309, doi:[10.1016/j.conbuildmat.2017.07.215](https://doi.org/10.1016/j.conbuildmat.2017.07.215)
- [6] He, C.-H.; Liu, H.-W.; Liu, C. (2024). A fractal-based approach to the mechanical properties of recycled aggregate concretes, *Facta Universitatis, Series: Mechanical Engineering*, Vol. 22, No. 2, 329-342, doi:[10.22190/FUME240605035H](https://doi.org/10.22190/FUME240605035H)
- [7] Awan, H. H.; Javed, M. F.; Yousaf, A.; Aslam, F.; Alabduljabbar, H.; Mosavi, A. (2021). Experimental evaluation of untreated and pretreated crumb rubber used in concrete, *Crystals*, Vol. 11, No. 5, Paper 558, 14 pages, doi:[10.3390/cryst11050558](https://doi.org/10.3390/cryst11050558)
- [8] Azunna, S. U.; Aziz, F. N. A. A.; Rashid, R. S. M.; Bakar, N. B. A. (2024). Review on the characteristic properties of crumb rubber concrete, *Cleaner Materials*, Vol. 12, Paper 100237, 33 pages, doi:[10.1016/j.clema.2024.100237](https://doi.org/10.1016/j.clema.2024.100237)

- [9] Roychand, R.; Gravina, R. J.; Zhuge, Y.; Ma, X.; Youssf, O.; Mills, J. E. (2020). A comprehensive review on the mechanical properties of waste tire rubber concrete, *Construction and Building Materials*, Vol. 237, Paper 117651, 20 pages, doi:[10.1016/j.conbuildmat.2019.117651](https://doi.org/10.1016/j.conbuildmat.2019.117651)
- [10] Marie, I. (2017). Thermal conductivity of hybrid recycled aggregate – rubberized concrete, *Construction and Building Materials*, Vol. 133, 516-524, doi:[10.1016/j.conbuildmat.2016.12.113](https://doi.org/10.1016/j.conbuildmat.2016.12.113)
- [11] Amiri, M.; Hatami, F.; Golafshani, E. M. (2021). Evaluating the synergic effect of waste rubber powder and recycled concrete aggregate on mechanical properties and durability of concrete, *Case Studies in Construction Materials*, Vol. 15, Paper e00639, 18 pages, doi:[10.1016/j.cscm.2021.e00639](https://doi.org/10.1016/j.cscm.2021.e00639)
- [12] Koh, T.; Shin, M.; Bae, Y.; Hwang, S. (2016). Structural performances of an eco-friendly prestressed concrete sleeper, *Construction and Building Materials*, Vol. 102, Part 1, 445-454, doi:[10.1016/j.conbuildmat.2015.10.189](https://doi.org/10.1016/j.conbuildmat.2015.10.189)
- [13] Gonzalez-Corominas, A.; Etxeberria, M.; Fernandez, I. (2017). Structural behaviour of prestressed concrete sleepers produced with high performance recycled aggregate concrete, *Materials and Structures*, Vol. 50, No. 1, Paper 94, 14 pages, doi:[10.1617/s11527-016-0966-6](https://doi.org/10.1617/s11527-016-0966-6)
- [14] Bae, Y.; Pyo, S. (2020). Ultra high performance concrete (UHPC) sleeper: structural design and performance, *Engineering Structures*, Vol. 210, Paper 110374, 14 pages, doi:[10.1016/j.engstruct.2020.110374](https://doi.org/10.1016/j.engstruct.2020.110374)
- [15] Kaewunruen, S.; Li, D.; Chen, Y.; Xiang, Z. (2018). Enhancement of dynamic damping in eco-friendly railway concrete sleepers using waste-tyre crumb rubber, *Materials*, Vol. 11, No. 7, Paper 1169, 20 pages, doi:[10.3390/ma11071169](https://doi.org/10.3390/ma11071169)
- [16] Kaewunruen, S.; Meesit, R. (2020). Eco-friendly high-strength concrete engineered by micro crumb rubber from recycled tires and plastics for railway components, *Advances in Civil Engineering Materials*, Vol. 9, No. 1, 210-226, doi:[10.1520/ACEM20180058](https://doi.org/10.1520/ACEM20180058)
- [17] Eller, B.; Fischer, S. (2025). Application of concrete canvas for enhancing railway substructure performance under static and dynamic loads, *Facta Universitatis, Series: Mechanical Engineering*, Online First, 27 pages, doi:[10.22190/FUME241129002E](https://doi.org/10.22190/FUME241129002E)
- [18] Xie, J.-H.; Guo, Y.-C.; Liu, L.-S.; Xie, Z.-H. (2015). Compressive and flexural behaviours of a new steel-fibre-reinforced recycled aggregate concrete with crumb rubber, *Construction and Building Materials*, Vol. 79, 263-272, doi:[10.1016/j.conbuildmat.2015.01.036](https://doi.org/10.1016/j.conbuildmat.2015.01.036)
- [19] Ali Ahmed, D.; Bahroz Jumaa, G.; Khalighi, M. (2022). Mechanical properties and shear strength of rubberized fibrous reinforced concrete beams without stirrups, *Construction and Building Materials*, Vol. 350, Paper 128796, 18 pages, doi:[10.1016/j.conbuildmat.2022.128796](https://doi.org/10.1016/j.conbuildmat.2022.128796)
- [20] Duan, F.; Zhu, H.; Ibrahim, Y. E.; Adamu, M. (2022). Durability and property study of decade old crumb rubber concrete cored specimens, *Materials*, Vol. 15, No. 16, Paper 5490, 13 pages, doi:[10.3390/ma15165490](https://doi.org/10.3390/ma15165490)
- [21] Assaggaf, R. A.; Ali, M. R.; Al-Dulaijan, S. U.; Maslehuddin, M. (2021). Properties of concrete with untreated and treated crumb rubber – a review, *Journal of Materials Research and Technology*, Vol. 11, 1753-1798, doi:[10.1016/j.jmrt.2021.02.019](https://doi.org/10.1016/j.jmrt.2021.02.019)
- [22] Wu, D.; Zhao, C. L.; Huang, C. L.; Luo, X. (2025). Micro-texture optimization for titanium cutting tools via simulation, *International Journal of Simulation Modelling*, Vol. 24, No. 2, 333-344, doi:[10.2507/IJSIMM24-2-CO7](https://doi.org/10.2507/IJSIMM24-2-CO7)
- [23] Liu, Z.; Jiang, Y.; Wang, T.; He, J. (2025). Neural network identification of the parameters of ultra-high-performance concrete bridges, *Technical Gazette*, Vol. 32, No. 4, 1383-1389, doi:[10.17559/TV-20250312002461](https://doi.org/10.17559/TV-20250312002461)
- [24] Gravina, R. J.; Xie, T. (2022). Toward the development of sustainable concrete with crumb rubber: design-oriented models, life-cycle-assessment and a site application, *Construction and Building Materials*, Vol. 315, Paper 125565, 16 pages, doi:[10.1016/j.conbuildmat.2021.125565](https://doi.org/10.1016/j.conbuildmat.2021.125565)